

Design, Synthesis and Pharmacological Evaluation of 5-Hydroxytryptamine_{1A} Receptor Ligands to Explore the Three-Dimensional Structure of the Receptor

MARÍA L. LÓPEZ-RODRÍGUEZ, BRUNO VICENTE, XAVIER DEUPI, SERGIO BARRONDO, MIREIA OLIVELLA, M. JOSÉ MORCILLO, BELLINDA BEHAMÚ, JUAN A. BALLESTEROS, JOAN SALLÉS, and LEONARDO PARDO

Departamento de Química Orgánica I, Facultad de Ciencias Químicas, Universidad Complutense, Madrid, Spain (M.L.L.-R., B.V., B.B.); Laboratori de Medicina Computacional, Unitat de Bioestadística, Facultat de Medicina, Universitat Autònoma de Barcelona, Barcelona, Spain (X.D., M.O., L.P.); Departamento de Farmacología, Universidad del País Vasco, Vitoria, Spain (S.B., J.S.); Facultad de Ciencias, Universidad Nacional de Educación a Distancia, Madrid, Spain (M.J.M.); and Novasite Pharmaceuticals, Inc., San Diego, California (J.A.B.)

Received September 27, 2001; accepted March 21, 2002

This article is available online at <http://molpharm.aspetjournals.org>

ABSTRACT

In this work, we evaluate the structural differences of transmembrane helix 3 in rhodopsin and the 5-hydroxytryptamine 1A (5-HT_{1A}) receptor caused by their different amino acid sequence. Molecular dynamics simulations of helix 3 in the 5-HT_{1A} receptor tends to bend toward helix 5, in sharp contrast to helix 3 in rhodopsin, which is properly located within the position observed in the crystal structure. The relocation of the central helix 3 in the helical bundle facilitates the experimentally derived interactions between the neurotransmitters and the Asp residue in helix 3 and the Ser/Thr residues in helix 5. The different amino acid sequence that forms helix 3 in rhodopsin (basically the conserved Gly^{3.36}Glu^{3.37} motif in the opsin family) and the 5-HT_{1A} receptor (the conserved Cys^{3.36}Thr^{3.37} motif in the neurotransmitter family) produces these structural diver-

gences. These structural differences were experimentally checked by designing and testing ligands that contain comparable functional groups but at different interatomic distance. We have estimated the position of helix 3 relative to the other helices by systematically changing the distance between the functional groups of the ligands (**1** and **2**) that interact with the residues in the receptor. Thus, ligand **1** optimally interacts with a model of the 5-HT_{1A} receptor that matches rhodopsin template, whereas ligand **2** optimally interacts with a model that possesses the proposed conformation of helix 3. The lack of affinity of **1** ($K_i > 10,000$ nM) and the high affinity of **2** ($K_i = 24$ nM) for the 5-HT_{1A} receptor binding sites, provide experimental support to the proposed structural divergences of helix 3 between the 5-HT_{1A} receptor and rhodopsin.

G protein-coupled receptors (GPCRs) are membrane proteins that transmit extracellular signals of neurotransmitters, peptides, and glycoproteins through heterotrimeric G proteins bound in the interior of the cell (Ji et al., 1998). The GPCR family possesses highly conserved motifs in the transmembrane region (Ballesteros and Weinstein, 1995; Horn et al., 1998), which suggests a common transmembrane structure. Recently, the detailed three-dimensional (3-D) structure of the GPCR rhodopsin (RHO) was determined at 2.8-Å resolution (Palczewski et al., 2000). This structure has confirmed that RHO and probably the RHO family of GPCRs are formed by a highly organized heptahelical transmembrane bundle. This structural homology between RHO and the other GPCRs probably does not extend to the extracellular

domain, for which there is very little homology, and is highly structured in RHO, blocking the access of the extracellular ligand to the core of the receptor (Bourne and Meng, 2000).

The amino acid residues involved in ligand binding have been primarily identified by pharmacological and mutagenesis studies [for review, see van Rhee and Jacobson (1996)]. In particular, agonists and antagonists of the neurotransmitter subfamily of GPCRs bind with their protonated amine to the conserved Asp^{3.32} (see *Materials and Methods* for the receptor-numbering scheme), in transmembrane helix (TMH) 3 (Strader et al., 1988). The hydroxyl groups present in the chemical structure of many neurotransmitters seem to hydrogen bond (Strader et al., 1989; Liapakis et al., 2000) a series of conserved Ser/Thr residues (5.42, 5.43, and 5.46), in TMH 5. Moreover, mutagenesis experiments on the α_2 - (Suryanarayana et al., 1991), β_2 - (Suryanarayana and Kobilka, 1993), 5-HT_{1A} (Guan et al., 1992), and 5-HT_{1B} (Glennon et al., 1996) receptors have shown that Asn^{7.39}, in TMH

This work was supported in part by grants from Dirección General de Investigación Científica y Tecnológica (PB97-0282), Comisión Interministerial de Ciencia y Tecnológica (SAF98-0064-C02 and SAF99-0073), Comunidad de Madrid (08.5/0079/2000), Universidad del País Vasco (G15/98), and Fundación La Marató TV3 (0014/97).

ABBREVIATIONS: GPCRs, G protein coupled receptors; 3-D, three-dimensional; RHO, rhodopsin; TMH, transmembrane helix; 5-HT_{1A}R, 5-hydroxytryptamine_{1A} receptor; EF-7412, 2-[4-[4(m-ethylsulfonamido)-phenyl]piperazin-1-yl]butyl]-1,3-dioxoperhydroppyrolo[1,2-c]imidazole.

7, is important in conferring specificity to a series of ligands such as pindolol and propranolol.

The publication of the crystal structure of RHO has provided the arrangement of the TMHs in the cell membrane (Palczewski et al., 2000). The central TMH 3 is near TMH 5 in its cytoplasmic end and far from TMH 5 in its extracellular end, which hinders the binding of the small neurotransmitter molecules between Asp^{3.32} and the implicated Ser/Thr^{5.42,5.43,5.46} residues, located at the extracellular side. This finding was previously noted in the translation of the electron density maps of frog RHO (Unger et al., 1997) into an α -carbon template (Baldwin et al., 1997). Thus, the following factor should be taken into account. Wide ranges of extracellular ligands, from small neurotransmitters to large peptides and hormones, are recognized by the different GPCR subfamilies. Each subfamily has probably developed specific structural motifs that allow the receptor to accommodate the different extracellular ligands. Interestingly, RHO possesses two non-conserved successive Gly residues at positions 89 (Gly^{2.56}) and 90 (Gly^{2.57}). This specific motif of the opsin family induces a significant distortion of TMH 2, which bends strongly toward TMH 1 (Palczewski et al., 2000). In contrast, the chemokine family of GPCR possesses in this region of TMH 2 a conserved Thr^{2.56}XPro^{2.58} motif, where X is any amino acid. We have recently shown that this TxP motif in CCR5 bends TMH 2 toward the center of the bundle and away from TMH 1 (Govaerts et al., 2001a). Moreover, this structural singularity is important for chemokine-induced functional response (Govaerts et al., 2001a). Thus, the presence of specific and conserved residues among the families of GPCR may result in structural differences among them. The similarities and differences between RHO and other GPCRs have recently been reviewed in detail (Ballesteros et al., 2001).

In this work, we aim to evaluate the structural differences of TMH 3 in RHO and the 5-HT_{1A} receptor (5-HT_{1A}R) caused by their different amino acid sequence. The conformation of TMH 3 in the neurotransmitter family of GPCR changes the location of Asp^{3.32} and in consequence where the extracellular ligand is placed. Thus, we aim to estimate the position of TMH 3 relative to the other helices, primarily TMH 5 and 7 where ligands bind, in the inactive conformation of the 5-HT_{1A}R. Several approaches have been developed to elucidate intermolecular distances between helices: double revertant mutant constructs (Zhou et al., 1994), spin labeling (Yang et al., 1996), zinc site engineering (Elling et al., 1995, 1999), and Cys crosslinking (Yu et al., 1995). We have developed a new approach in which the distance between the functional groups of the ligand that interact with the residues in the receptor is systematically varied. This procedure has allowed us to discern between conformations of the receptor obtained computationally. Antagonists are preferred over agonists to explore the inactive form of the receptor. Recently, we have reported the pharmacological characterization of EF-7412 as an antagonist in vivo in pre- and postsynaptic 5-HT_{1A}R sites (Lopez-Rodríguez et al., 2001a,b). We have designed, synthesized, and pharmacologically evaluated a new set of compounds, using EF-7412 as a template, to discern between computer models of the 5-HT_{1A}R.

Materials and Methods

Residue Numbering Scheme. Each transmembrane residue is numbered with the helix number (from 1 to 7) in which it is located plus its relative position to the most conserved residue in the helix, arbitrarily labeled 50 (Ballesteros and Weinstein, 1995). Therefore, the most conserved TMH 3 residue is designated with the index number 3.50 (Arg^{3.50}). The Asp preceding the Arg in the (D/E)RY motif is designated Asp^{3.49}, and the Tyr after the Arg is designated Tyr^{3.51}.

Molecular Dynamics Simulations of TMH 3 in RHO and the 5-HT_{1A}R. The peptide corresponding to the residues from 3.22 to 3.54 in TMH 3 of RHO (Ace-PTGCFYFEGFFATLGGELALWLSLVV-LAIERYVVV-NMe), and the 5-HT_{1A}R (Ace-QVTCDFIALDVL-CCTSSILHLCAIALDRYWAI-NMe), were built in the standard α -helix conformation (backbone dihedral angles ϕ and ψ of -58 and -47 degrees). All ionizable residues in the helices were considered uncharged. The structures obtained were placed in a rectangular box containing methane molecules (2693 and 3095 for RHO and 5-HT_{1A}R, respectively) to mimic the hydrophobic environment of the TMHs. A similar procedure has recently been employed to mimic the membrane in molecular dynamics simulations of the thyrotropin receptor (Govaerts et al., 2001b) and TMH 2 of the CCR5 receptor (Govaerts et al., 2001a). The sizes of the boxes were $74.5 \times 43.5 \times 41.0$ Å for RHO, and $76.5 \times 45.5 \times 41.5$ Å for 5-HT_{1A}R. The systems were energy-minimized (500 steps), heated (from 0 to 300°K in 15 ps), equilibrated (from 15 to 500 ps) and the production run (from 500 to 1000 ps) was carried out at constant volume using the particle mesh Ewald method to evaluate electrostatic interactions. Structures were collected every 5 ps during the last 500 ps of simulation (100 structures per simulation). The molecular dynamics simulations were run with the Sander module of AMBER 5 (<http://www.amber.ucsf.edu/amber/amber.html>), the all-atom force field (Cornell et al., 1995), SHAKE bond constraints in all bonds, a 2-fs integration time step, and constant temperature of 300°K coupled to a heat bath.

The logistic regression model (Hosmer and Lemeshow, 1989) was used to fit the binary dependent variable (RHO, 5-HT_{1A}R) to the independent variables: the torsional angles (ϕ and ψ) of the residues spanning from 3.33 to 3.48 (32 variables) obtained during the molecular dynamics trajectory (a total of 200 structures). In contrast to the standard regression analysis, the dependent variable in the logistic regression is discrete, taking only two possible values (RHO and 5-HT_{1A}R). The stepwise method was employed to select the independent variables in the model. Thus, only the torsional angles ϕ and ψ that better classify the structures as RHO or 5-HT_{1A}R are included in the regression equation. The odds ratio is a function of the coefficient of the independent variable in the regression equation and measures how many times it is more likely to be RHO or 5-HT_{1A}R with a decrease or an increase of 1° in the torsional angles (independent variables). The larger the value of the odds ratio, the more predictive the independent variable is. Independent variables with odds ratio of 1 indicates no predictive power. Calculations were performed with SAS 6.11 (SAS Institute, Cary, NC).

A Molecular Model of the 5-HT_{1A}R. The 3-D model of the transmembrane domain of the 5-HT_{1A}R was constructed by computer-aided model building techniques from the crystal structure of RHO (Palczewski et al., 2000) (PDB access number 1F88). Conserved residues Asn⁵⁵ (residue number in the PDB file of RHO) and Asn⁵⁴ (residue number in the human 5-HT_{1A}R sequence) [Asn^{1.50} in the generalized numbering scheme (Ballesteros and Weinstein, 1995)]; Asp⁸³ and Asp⁸² (Asp^{2.50}); Arg¹³⁵ and Arg¹³⁴ (Arg^{3.50}); Trp¹⁶¹ and Trp¹⁶¹ (Trp^{4.50}); Pro²¹⁵ and Pro²⁰⁷ (Pro^{5.50}); Pro²⁶⁷ and Pro³⁶⁰ (Pro^{6.50}); and Pro³⁰³ and Pro³⁹⁷ (Pro^{7.50}) were employed in the alignment of RHO and human 5-HT_{1A}R transmembrane sequences. All ionizable residues in the helices were considered uncharged with the exception of Asp^{2.50}, Asp^{3.32}, Asp^{3.49}, Arg^{3.50}, and Glu^{6.30}. SCWRL-2.1 was employed to add the side chains of the nonconserved residues based on a backbone-dependent rotamer library (Dunbrack and Co-

hen, 1997). This computer model, which maintains the position of the TMHs as in RHO, is denoted 5-HT_{1A}R^{RHO}. TMH 3 was then replaced by the most representative structure of the geometries obtained during the molecular dynamics trajectory of TMH 3 in 5-HT_{1A}R (see above). This representative structure was selected by automatically clustering the collected geometries into conformationally related subfamilies with the program NMRCCLUS (Kelley et al., 1996). The backbone of the highly conserved E/DR^{3.50Y} motif superimposed the structures. This computer model, which changes relative to 5-HT_{1A}R^{RHO} the position of TMH 3 at the extracellular side, is denoted 5-HT_{1A}R^{MD}.

The initial structure of the complex between (±)-2-[4-[4-(6-hydroxy-2-pyridyl)piperazin-1-yl]butyl]-1,3-dioxoperhydropyrrolo[1,2-c]imidazole (**1**) and (±)-2-[4-[4-(*m*-acetylaminophenyl)piperazin-1-yl]butyl]-1,3-dioxoperhydropyrrolo[1,2-c]imidazole (**2**) and the 5-HT_{1A}R was obtained from the previously reported structure of the complex between EF-7412 and the 5-HT_{1A}R (Lopez-Rodriguez et al., 2001b). Subsequently, the complete systems were energy-minimized (5000 steps). Energy minimizations were run with the Sander module of AMBER 5 (<http://www.amber.ucsf.edu/amber/amber.html>), the all-atom force field (Cornell et al., 1995), and a 13-Å cutoff for nonbonded interactions. Parameters for ligands **1** and **2** were adapted from the force field of Cornell et al. (1995) using RESP point charges (Cieplak et al., 1995).

Chemistry. Derivative **1** was synthesized by the following procedure: 2.0 ml of triethylamine (1.5 g, 14.6 mmol) was added to a suspension of 2.5 g (9 mmol) of 2-(4-bromobutyl)-1,3-dioxoperhydropyrrolo[1,2-c]imidazole (Lopez-Rodriguez et al., 1996) and 2.7 g (15 mmol) of 1-(6-hydroxy-2-pyridyl)piperazine (Pavia et al., 1987) in 19 ml of acetonitrile. The mixture was refluxed for 20 to 24 h (thin-layer chromatography). Then, the solvent was evaporated under reduced pressure and the residue was resuspended in water and extracted with dichloromethane (3 × 100 ml). The combined organic layers were washed with water and dried over MgSO₄. After evaporation of the solvent, the crude oil was purified by column chromatography (dichloromethane) to afford 1.1 g (33%) of **1**, which was converted into the hydrochloride salt. Derivative **2** was synthesized by the following procedure: 0.11 ml (1.6 mmol) of acetyl chloride was added dropwise to a solution of 600 mg (1.6 mmol) of 2-[4-[4-(*m*-aminophenyl)piperazin-1-yl]butyl]-1,3-dioxoperhydropyrrolo[1,2-c]imidazole (Lopez-Rodriguez et al., 2001a) in 20 ml of pyridine at 0°C. After stirring at room temperature for 1.5 h (thin-layer chromatography), the mixture was diluted with 50 ml of methylene chloride and washed with a saturated aqueous solution of CuSO₄, water, and brine (25 ml). The organic layer was dried (Na₂SO₄) and the solvent evaporated under reduced pressure to afford 668 mg (67%) of **2**, which was converted to the hydrochloride salt. The new compounds were characterized by IR and ¹H- and ¹³C-NMR spectroscopy and gave satisfactory combustion analyses (C, H, N).

Radioligand Binding Assays. The 5-HT_{1A} receptor binding studies were performed by a modification of a procedure described previously (Clark et al., 1990). The cerebral cortices of male Sprague-Dawley rats (*Rattus norvegicus albinus*) weighing 180 to 200 g were homogenized in 10 volumes of ice-cold Tris buffer (50 mM Tris-HCl, pH 7.7 at 25°C) and centrifuged at 28,000g for 15 min. The membrane pellet was washed twice by resuspension and centrifugation. After the second wash, the resuspended pellet was incubated at 37°C for 10 min. Membranes were then collected by centrifugation and the final pellet was resuspended in 50 mM Tris-HCl, 5 mM MgSO₄, and 0.5 mM EDTA buffer, pH 7.4 at 37°C. Fractions of the final membrane suspension (about 1 mg of protein) were incubated at 37°C for 15 min with 0.6 nM [³H]8-hydroxy-2-dipropylaminotetralin (133 Ci/mmol), in the presence or absence of several concentrations of the competing drug, in a final volume of 1.1 ml of assay buffer (50 mM Tris-HCl, 10 nM clonidine, 30 nM prazosin, pH 7.4 at 37°C). Incubation was terminated by rapid vacuum filtration through Whatman GF/B filters, presoaked in 0.05% poly(ethylenimine), using a Brandel cell harvester. The filters were then washed with the assay buffer

and dried. The filters were placed in poly(ethylene) vials to which 4 ml of a scintillation cocktail (Aquasol) was added, and the radioactivity bound to the filters was measured by liquid scintillation spectrometry. The data were analyzed by an iterative curve-fitting procedure (Prism; GraphPad Software, San Diego, CA), which provided IC₅₀, K_i, and r² values for test compounds; K_i values were calculated from the Cheng and Prusoff equation (Cheng and Prusoff, 1973). The protein concentrations of the rat cerebral cortex were determined by the method of Lowry et al. (1951) using bovine serum albumin as the standard. Nonspecific binding was determined with 10 μM 5-HT. Competing drug, nonspecific, total and radioligand bindings were defined in triplicate.

Results and Discussion

Amino Acid Composition of TMH 3 in the Opsin and Neurotransmitter Families of GPCR. We analyze in this section the amino acid sequence of TMH 3 in the opsin and neurotransmitter families that might cause structural differences in the helix. These differences are relevant because the crystal structure of RHO (Palczewski et al., 2000) is an appropriate template to model the 3-D structure of receptors for neurotransmitters and the conformation of TMH 3 in the neurotransmitter family changes the location of Asp^{3.32}, the anchoring point of both agonists and antagonists (Strader et al., 1988; van Rhee and Jacobson, 1996). The intracellular side of TMH 3 contains in both cases the highly conserved E/DR^{3.50Y} motif. The protonation of E/D^{3.49} is thought to be important in G-protein coupling (Arnis et al., 1994; Oliveira et al., 1994; Scheer et al., 1996). We assume that this common E/DR^{3.50Y} motif, in the compact cytoplasmatic surface, is held in similar position in both families. Thus, the location of the amino acid 3.32 in the opsin and the neurotransmitter families, relative to the E/DR^{3.50Y} motif, will depend on the amino acid composition of the residues spanning from 3.33 to 3.48.

Table 1 shows the statistical analysis of the conservation pattern in this continuous stretch of residues from 3.33 to 3.48 of all GPCR sequences denoted as (Rhod)opsin (245 entries) and Amine (288 entries) in GPCRDB (Horn et al., 1998), as of December 2001. Ser or Thr or Cys residues are present in 6 of 16 positions (3.35, 3.36, 3.37, 3.39, 3.44, and

TABLE 1

Statistical analysis of the conservation pattern in a continuous stretch of residues from 3.33 to 3.48 in TMH 3 of all GPCR sequences denoted as (Rhod)opsin and Amine in GPCRDB.

The position in the helix, the amino acid most often present at this position, and the population of this amino acid in the family are shown.

Position	(Rhod)opsin	Amine
	%	
3.33	Thr 51.4	Val 64.6
3.34	Leu 65.7	Leu 51.0
3.35	Gly 50.0	Cys 53.1
3.36	Gly 98.8	Cys 56.9
3.37	Glu 34.3	Thr 85.1
3.38	Ile 33.1	Ala 82.6
3.39	Ala 41.2	Ser 100.0
3.40	Leu 66.9	Ile 85.8
3.41	Trp 85.3	Leu 43.4
3.42	Ser 77.1	Asn 42.4
3.43	Leu 80.4	Leu 89.9
3.44	Val 40.8	Cys 72.6
3.45	Val 55.5	Ala 41.7
3.46	Leu 54.3	Ile 92.1
3.47	Ala 75.9	Ser 65.3
3.48	Ile 33.5	Leu 42.0

3.47) more than 50% of the time in the neurotransmitter family, in sharp contrast to the opsin family, which contains only two positions (3.33 and 3.42). Ser, Thr, and Cys residues play a special role in α -helices because they can form an intrahelical hydrogen bond between the side chain OH _{γ} (or SH _{γ}) and the i-3 or i-4 carbonyl oxygen of the preceding turn (Gray and Matthews, 1984). This additional hydrogen bond to the peptide carbonyl oxygen can produce significant changes in the curvature of the helix (Ballesteros et al., 2000; Govaerts et al., 2001a). It is important to note that Ser, Thr, and Cys are not present simultaneously in the opsin and the neurotransmitter families in the 3.33–3.48 range (Table 1). Besides, there are two amino acid sites in the TMH 3 domain of the opsin family at which a Gly is present in more than 50% of the receptors: Gly^{3.35} (50.0%) and Gly^{3.36} (98.8%). Gly is most often located in loop regions and acts as helix-breaker in soluble proteins (O’Neil and DeGrado, 1990). In contrast, Gly residues are frequently detected in the transmembrane segments of membrane proteins (Senes et al., 2000) which suggests a structural role. The absence of the side chain in Gly probably adds flexibility to Gly-containing helices (Kumar and Bansal, 1998). The neurotransmitter family possesses Cys residues at these 3.35 and 3.36 positions. Thus, the different attributes of the amino acids forming TMH 3 in the opsin and the neurotransmitter families can produce significant structural deviations among them.

Molecular Dynamics Simulations of TMH 3 in RHO and the 5-HT_{1A}R. To obtain a rough idea of the possible consequences that the different amino acid sequences that form TMH 3 in rhodopsin and the 5-HT_{1A}R might have on the structure, we performed a molecular modeling exercise using the 3-D structure of rhodopsin as the template (Palczewski et al., 2000). Figure 1, a (view parallel to the membrane with the extracellular side at the top) and b (perpendicular to the membrane from the extracellular side), show the result of superimposing the structures computed during the molecular dynamics trajectory (see *Materials and Methods* for computational details) of the amino acid sequence that form TMH 3 in RHO (orange) and the 5-HT_{1A}R (green) on TMH 3 of RHO. The backbone of the highly conserved E/DR^{3.50}Y motif superimposed the computed structures and the helix bundle of RHO. This procedure hypothesizes that the common E/DR^{3.50}Y motif is located in similar positions in rhodopsin and the 5-HT_{1A}R. Visual inspection of the helix axes of the computed structures in Fig. 1, a and b, reveal that TMH 3 in RHO and the 5-HT_{1A}R behaves differently. The conformational space explored by the extracellular part of TMH 3 in the 5-HT_{1A}R is precisely toward TMH 5. In contrast, the energetically available structures of RHO are distant to TMH 5, basically within the position of TMH 3 in the crystal structure.

The logistic regression model (see *Materials and Methods* for computational details) was employed to characterize the amino acid positions in RHO and the 5-HT_{1A}R that most influence the structural differences observed in TMH 3. The binary dependent variable (RHO, 5-HT_{1A}R) was fitted to the torsional angles (Φ and Ψ) of the residues spanning from 3.33 to 3.48. Table 2 shows the torsional angles selected in the stepwise procedure and the odds ratio of the included variables. The torsional angles Φ of the residue at position 3.35 ($\Phi_{3.35}$); Φ and Ψ at positions 3.36 and 3.37 ($\Phi_{3.36}$, $\Phi_{3.37}$, $\Psi_{3.36}$, and $\Psi_{3.37}$); and Ψ at positions 3.39, 3.43, and 3.46 ($\Psi_{3.39}$,

$\Psi_{3.43}$, and $\Psi_{3.46}$), properly classify 100% of the input conformations of RHO and the 5-HT_{1A}R. However, the predictive power of the selected torsions is not the same. The variables $\Phi_{3.36}$, $\Phi_{3.37}$, $\Psi_{3.36}$, and $\Psi_{3.37}$ possess the highest odds ratio (Table 2) and thus the highest classification power. A logistic regression model with only these four independent variables

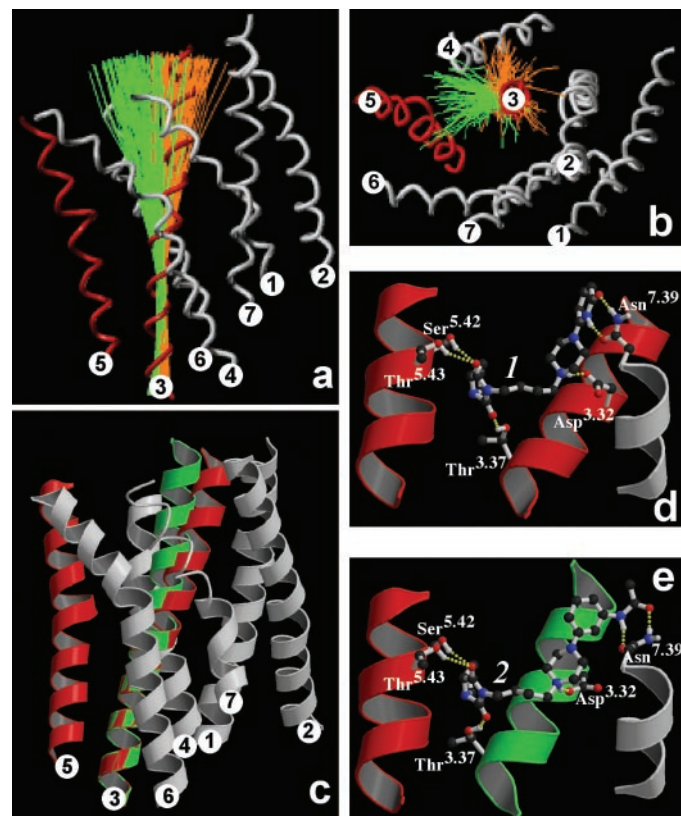


Fig. 1. a and b, the α -carbon traces of the transmembrane helix bundle of RHO (Palczewski et al., 2000) are depicted as tube ribbons in red for TMHs 3 and 5 and white for the other TMHs. The views are parallel to the membrane with the extracellular side at the top (a) and perpendicular to the membrane from the extracellular side (b). The helix axes of the structures computed during the molecular dynamics trajectory of the amino acid sequence that form TMH 3 in RHO (orange) and the 5-HT_{1A}R (green) are displayed. c, the representative structure of the geometries obtained during the molecular dynamics trajectory of TMH 3 in the 5-HT_{1A}R (green helix axes) is shown in green. d and e, detailed view of the transmembrane helix bundle of 5-HT_{1A}R^{RHO} complexed with ligand **1** (d) and 5-HT_{1A}R^{RMD} complexed with ligand **2** (e). The C α traces of the extracellular part (top) of TM 3, 5, and 7 are only shown. Nonpolar hydrogens are not depicted to offer a better view of the recognition pocket. Figures were created using MolScript ver. 2.1.1 (Kraulis, 1991) and Raster3D ver. 2.5 (Merritt and Bacon, 1997).

TABLE 2

Torsional angles and its odds ratio of the selected variables in the stepwise logistic regression between the binary dependent variable (RHO, 5-HT_{1A}R) and the torsional angles (Φ and Ψ) obtained during the molecular dynamics trajectory of the residues spanning from 3.33 to 3.48.

Torsion _{Position}	Odds ratio
$\Phi_{3.35}$	2.0
$\Phi_{3.36}$	4.5
$\Psi_{3.36}$	5.0
$\Phi_{3.37}$	2.3
$\Psi_{3.37}$	2.9
$\Psi_{3.39}$	1.7
$\Psi_{3.43}$	1.4
$\Psi_{3.46}$	1.7

already classifies 93% of the input conformations. Remarkably, Gly^{3.36} is highly conserved in the opsin family (98.8%) but not in the neurotransmitter family that contains Cys (56.9%). Substitution of Gly^{3.36} in RHO with more bulky residues promotes partial agonist activity of 11-*cis*-retinal (Han et al., 1997). Thr^{3.37} is present 85.1% of the time in the neurotransmitter family and is absent in the opsin family (Glu 34.3%, Ile 21.8%). It is important to note that Thr^{3.37} is not present in the 5-HT₆ and muscarinic receptor subfamilies (see *Conclusions*). Substitution of Thr^{3.37} in the α_{1B} -adrenergic receptor by Ala produces epinephrine and norepinephrine to behave as partial agonists (Cavalli et al., 1996). The same authors concluded that Thr^{3.37} might play a role in preserving the receptor structure and function rather than directly interacting with the agonist (Cavalli et al., 1996).

We propose that the different structural properties of Gly^{3.36}Glu^{3.37} in the opsin family and Cys^{3.36}Thr^{3.37} in the neurotransmitter family produce different TMH 3 orientations. This results in structural divergences between the neurotransmitter family of GPCR and RHO template (Palczewski et al., 2000). The absence of Thr^{3.37} in the muscarinic receptors also suggests structural divergences relative to the other members of the neurotransmitter family. Incorporation into the RHO template (white and red transmembrane helix bundle in Fig. 1c) of a representative conformation of TMH 3 (green transmembrane helix in Fig. 1c; see *Materials and Methods* for computational details) results in a significant displacement of Asp^{3.32} toward TMH 5, without modifying the more compact cytoplasmatic surface. This relocation facilitates the experimentally derived interactions between the neurotransmitters and the Ser/Thr residues in TMH 5. In particular, Ser^{5.42} and Thr^{5.43} are important in the binding of agonists to the 5-HT_{1A}R (Ho et al., 1992). The magnitude of the relocation might be estimated from the structures depicted in Fig. 1c. Thus, the distances between the α -carbon positions of the implicated Asp^{3.32} and Ser^{5.42} and Thr^{5.43} residues in the RHO template (5-HT_{1A}R^{RHO}, see methods) are 14.6 and 15.9 Å, respectively. These distances decrease to 12.6 and 14.1 Å if the obtained conformation of TMH 3 from the 5HT_{1A}R is incorporated into the RHO template (5-HT_{1A}R^{MD}).

It must be stressed that there may be other structural variations that could facilitate the binding of neurotransmitter to their receptors. We must be open to the possibility that the different sequence of the other transmembrane helices might also cause structural differences as well. However, the conservation of functionally important sequence motifs within the rhodopsin-like GPCR family has been interpreted to mean that the basic characteristics of the rhodopsin fold are similar in the different receptor subtypes. We propose that structural adaptation of a receptor to its cognate ligand is necessary in some domains of the transmembrane region while still maintaining a similar overall rhodopsin fold. We hypothesize structural differences only in TMH 3, whereas the other transmembrane helices remain unchanged relative to the RHO template.

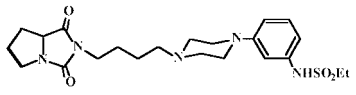
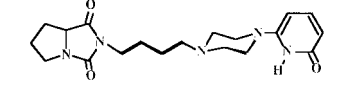
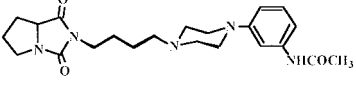
Design and Test of 5-HT_{1A}R Ligands That Interact with Asp^{3.32} and Asn^{7.39} to Discern between the Conformation of TMH 3. We aim to provide experimental support to the proposed conformation of TMH 3 by designing and testing 5-HT_{1A}R ligands that contain comparable functional groups but differ in the interatomic distance between them.

The rationale behind this approach is that by varying the distance between the functional groups of the ligand that interact with the side chains of the receptor, we will be able to discern between the computer models of TMH 3. EF-7412 (see Table 3), a recent pharmacologically characterized antagonist in vivo in pre- and postsynaptic 5-HT_{1A}R sites (Lopez-Rodriguez et al., 2001a), will be used as a template. It was proposed that EF-7412 forms an ionic interaction with Asp^{3.32} throughout the protonated amine of the piperazine ring, hydrogen bonds with Asn^{7.39} throughout the *m*-NHSO₂Et group, and hydrogen bonds with Thr^{3.37}, Ser^{5.42}, and Thr^{5.43} throughout the hydantoin moiety of the ligand (Lopez-Rodriguez et al., 2001b). A first approach would be to change the distance between the protonated amine of the piperazine ring and the hydantoin moiety of the ligand to assess the conformation of TMH 3 relative to TMH 5. However, the flexibility of the -CH₂ chain connecting both groups would impede to obtain any reliable conclusion. Nevertheless, the bending of TMH 3 toward TMH 5 also modifies the position of TMH 3 relative to TMH 7 at the extracellular site. Thus, we have designed 5-HT_{1A}R ligands that intended to interact with Asp^{3.32} and Asn^{7.39}, to discriminate the conformation of TMH 3 relative to TMH 7. Remarkably, these two positions have also been used to elucidate intermolecular distances by zinc site engineering experiments: substitution of Asp^{3.32} for His and Asn^{7.39} for Cys in the β_2 -adrenergic receptor results in a mutant that is activated by free zinc ions (Elling et al., 1999).

Table 3 shows the chemical structures of compounds **1** and **2**. These ligands replace the *m*-NHSO₂Et group of EF-7412 with a common -NHCO group that optimally interacts with the side chain of Asn^{7.39}. This -NHCO group is located at different positions in the structure relative to the protonated amine. The interatomic distance between the nitrogen of the protonated amine and the centroid of the -NHCO group for compounds **1** and **2** are 6.4 and 8.5 Å, respectively. Structures **1** and **2** were optimized (see *Materials and Methods* for computational details) inside 5-HT_{1A}R^{RHO} and 5-HT_{1A}R^{MD} models, respectively. Figure 1, d and e, show **1** and **2**, respectively, in the binding pocket. The unique N-H group of the protonated amine of both ligands interacts with one of the O_s atoms of Asp at the optimized distance between heteroatoms

TABLE 3

In vitro binding data of compounds EF-7412, **1**, and **2**
All values are the mean \pm S.E.M. of two to four experiments performed in triplicate.

Compound	5-HT _{1A} [³ H]8-OH-DPAT
	<i>nM</i>
	EF-7412 27 \pm 8
	1 > 10,000
	2 24 \pm 2

From Lopez-Rodriguez et al. (2001a, b).
8-OH-DPAT, 8-hydroxy-2-dipropylaminotetralin.

of 2.5 Å in both cases. Moreover, the N-H moiety of the common –NHCO group acts as a hydrogen bond donor in the hydrogen bond interaction with the O₈₁ atom of Asn, at the optimized distances between heteroatoms of 2.8 Å in both ligands, and the C=O moiety of –NHCO group acts as a hydrogen bond acceptor in the hydrogen bond interaction with the N₈₂-H moiety of Asn, at the optimized distances between heteroatoms of 2.8 or 2.9 Å for ligands **1** or **2**, respectively. Moreover, the proposed recognition of the extracellular ligands involves the hydrogen bonds between both C=O groups of the hydantoin moiety of the ligand and Thr^{3.37} (2.9 Å in both ligands), Ser^{5.42} (3.5 Å) and Thr^{5.43} (3.5 Å). Thus, **1** interacts optimally with 5-HT_{1A}R^{RHO}, which matches RHO template, whereas **2** optimally interacts with 5-HT_{1A}R^{MD}, which possesses the proposed conformation of TMH 3. It is important to note that the interaction of the –NHCO group of ligand **2** with Asn^{7.39} would benefit from a more bent conformation of TMH 3, which located the helix closer to TMH 5 and farther from TMH 7 at the extracellular part. This more extreme conformation was energetically accessible during the molecular dynamics trajectory of TMH 3 (see above). However, this conformational subfamily was not selected as the most representative in the automatic clustering procedure with the program NMRCLUST and was not used in the construction of 5-HT_{1A}R^{MD} (see *Materials and Methods*).

Table 3 shows the in vitro affinity of compounds **1** ($K_i > 10,000$ nM) and **2** ($K_i = 24$ nM) for the 5-HT_{1A}R binding sites. The lack of affinity of **1**, which was designed to match RHO template (5-HT_{1A}R^{RHO}), and the high affinity of **2**, which was designed to interact with a modified template of RHO (5-HT_{1A}R^{MD}), provides experimental support to the proposed structural divergences of TMH 3 between the 5-HT_{1A}R and RHO.

Conclusions

We have presented in this study a structural analysis of the conformation of TMH 3 in RHO and the 5-HT_{1A}R in the context of the crystal structure of RHO (Palczewski et al., 2000). This analysis is relevant because the structure of RHO is normally used as a template to model the class A family of GPCRs and the conformation of TMH 3 in the neurotransmitter family changes the location of Asp^{3.32}, the anchoring point of both agonists and antagonists (Strader et al., 1988; van Rhee and Jacobson, 1996). The different amino acid sequence of TMH 3 in RHO (basically the conserved Gly^{3.36}Glu^{3.37} motif in the opsin family) and the 5-HT_{1A}R (the conserved Cys^{3.36}Thr^{3.37} motif in the neurotransmitter family) produces significant structural divergences. Molecular dynamics simulations of the amino acid sequence that forms TMH 3 in the 5-HT_{1A}R tends to bend toward TMH 5, in sharp contrast to the amino acid sequence that forms TMH 3 in RHO, which is properly located within the position observed in the crystal structure. The relocation of the central TMH 3 facilitates the experimentally derived interactions between the neurotransmitters and the Asp residue in TMH 3 and the Ser/Thr residues in TMH 5.

We have designed two new ligands (**1** and **2**) that are thought to interact, in addition to other residues in the 5-HT_{1A}R, with Asp^{3.32} in TMH 3 and Asn^{7.39} in TMH 7. Ligand **1** interacts optimally with a model of the 5-HT_{1A}

receptor that matches rhodopsin template, whereas ligand **2** interacts optimally with a model that possesses the proposed conformation of helix 3. The lack of affinity of **1** ($K_i > 10,000$ nM) and the high affinity of **2** ($K_i = 24$ nM) for the 5-HT_{1A}R binding sites provides experimental support to the proposed structural divergences of helix 3 between the 5-HT_{1A}R and RHO. The significant difference in affinity ($K_i > 10000$ nM versus $K_i = 24$ nM) between these similar compounds that contain comparable functional groups led us to suggest that the 5-HT_{1A}R binding sites are not flexible and the extracellular ligand must be accommodated in the binding site in an optimal manner.

Statistical analysis of the conservation pattern at the 3.37 position shows that Thr (85.1%) is present in all the neurotransmitter family of GPCRs apart from the 5-HT₆ receptor which contains Ser (2.4%) and the muscarinic receptors which contains Asn (10.8%). All these polar side chains can form intrahelical hydrogen bonds with the backbone and bend helices (Ballesteros et al., 2000). There is more degree of variability across neurotransmitter receptors at the 3.36 locus. Cys (56.9%) is present in the α -adrenergic, dopamine (with the exception of D₁), histamine (with the exception of H₁), and serotonin (with the exception of 5-HT₂ and 5-HT₄) subfamilies of receptors; Ser (28.5%) is present in the D₁, H₁, 5-HT₂, and muscarinic receptors; Thr (1.7%) is present in the 5-HT₄ receptor; and Val (12.1%) is present in the β -adrenergic subfamily of receptors. The side chains of both Ser and Thr can form hydrogen bonds with the backbone (Ballesteros et al., 2000), the side chain of Cys can also form hydrogen bonds with the backbone but of less strength, and the non-polar side chain of Val cannot form hydrogen bonds. We have shown recently that the impairment of CCR5 receptor activation caused by the T82V, T82C, and T82S mutations parallels with the bending of the α -helix caused by these residues (Govaerts et al., 2001a). Thus, the presence of Thr, Ser, Cys, or Val alters to a greater or lesser degree the conformation of the helix. The wide range of bending and twisting that can result from the presence of these residues in TMH 3 has recently been illustrated (Ballesteros et al., 2001). These findings suggest that there might be some degree of variability in TMH 3 across the neurotransmitter family. Importantly, there are conservation patterns among subfamilies at the 3.36 and 3.37 positions. D₁, H₁, and 5-HT₂ receptors contain SerThr, 5-HT₄ receptors contain ThrThr, β -adrenergic receptors contain ValThr, 5-HT₆ receptors contain CysSer, muscarinic receptors contain SerAsn, and all the others contain CysThr. These findings might serve to model the complexes between the neurotransmitter family and their ligands. These models are important because they provide the tools for guiding the design and synthesis of new ligands with predetermined affinities and selectivity.

Acknowledgments

Computer facilities were provided by the Centre de Computació i Comunicacions de Catalunya.

References

- Arniss S, Fahmy K, Hofmann KP, and Sakmar TP (1994) A conserved carboxylic acid group mediates light-dependent proton uptake and signaling by rhodopsin. *J Biol Chem* **269**:23879–23881.
- Baldwin JM, Schertler GFX, and Unger VM (1997) An alpha-carbon template for the transmembrane helices in the rhodopsin family of G-protein-coupled receptors. *J Mol Biol* **272**:144–164.
- Ballesteros JA, Deupi X, Olivella M, Haaksma EEJ, and Pardo L (2000) Serine and

- threonine residues bend α -helices in the $\chi_1 = g_-$ conformation. *Biophys J* **79**:2754–2760.
- Ballesteros JA, Shi L, and Javitch JA (2001) Structural mimicry in G protein-coupled receptors: implications of the high-resolution structure of rhodopsin for structure-function analysis of rhodopsin-like receptors. *Mol Pharmacol* **60**:1–19.
- Ballesteros JA and Weinstein H (1995) Integrated methods for modeling G-protein coupled receptors. *Methods Neurosci* **25**:366–428.
- Bourne HR and Meng EC (2000) Structure. Rhodopsin sees the light. *Science (Wash DC)* **289**:733–734.
- Cavalli A, Fanelli F, Taddei C, De Benedetti PG, and Cotecchia S (1996) Amino acids of the α_{1B} -adrenergic receptor involved in agonist binding: differences in docking catecholamines to receptor subtypes. *FEBS Lett* **399**:9–13.
- Cheng YC and Prusoff WH (1973) Relationship between the inhibition constant (K_i) and the concentration of inhibitor which causes 50 per cent inhibition (IC_{50}) of an enzymatic reaction. *Biochem Pharmacol* **22**:3099–3108.
- Cieplak P, Cornell WD, Bayly C, and Kollman PA (1995) Application of the multi-molecule and multiconformational RESP methodology to biopolymers: charge derivation for DNA, RNA and proteins. *J Comput Chem* **16**:1357–1377.
- Clark RD, Weinhardt KK, Berger J, Fischer LE, Brown CM, MacKinnon A, Kilpatrick AT, and Spedding M (1990) 1,9-Alkano-bridged 2,3,4,5-tetrahydro-1H-3-benzazepines with affinity for the α_2 -adrenoceptor and the 5-HT_{1A} receptor. *J Med Chem* **33**:633–641.
- Cornell WD, Cieplak P, Bayly CI, Gould IR, Merz KM Jr, Ferguson DM, Spellmeyer DC, Fox T, Caldwell JW, and Kollman PA (1995) A second generation force field for the simulation of proteins, nucleic acids and organic molecules. *J Am Chem Soc* **117**:5179–5197.
- Dunbrack RLJ and Cohen FE (1997) Bayesian statistical analysis of protein sidechain rotamer preferences. *Protein Sci* **6**:1661–1681.
- Elling CE, Nielsen SM, and Schwartz TW (1995) Conversion of antagonist-binding site to metal-ion site in the tachykinin NK-1 receptor. *Nature (Lond)* **374**:74–77.
- Elling CE, Thirstrup K, Holst B, and Schwartz TW (1999) Conversion of agonist site to metal-ion chelator site in the β_2 -adrenergic receptor. *Proc Natl Acad Sci USA* **96**:12322–12327.
- Glennon RA, Dukat M, Westkaemper RB, Ismaiel AM, Izzarelli DG, and Parker EM (1996) The binding of propranolol at 5-hydroxytryptamine_{1D β} T355N mutant receptors may involve formation of two hydrogen bonds to asparagine. *Mol Pharmacol* **49**:198–206.
- Govaerts C, Blanpain C, Deupi X, Ballet S, Ballesteros JA, Wodak S, Vassart G, Pardo L, and Parmentier M (2001a) The TxP motif in the second transmembrane helix of CCR5: a structural determinant in chemokine-induced activation. *J Biol Chem* **276**:13217–13225.
- Govaerts C, Lefort A, Costagliola S, Wodak S, Ballesteros JA, Pardo L, and Vassart G (2001b) A conserved Asn in TM7 is a on/off switch in the activation of the TSH receptor. *J Biol Chem* **276**:22991–22999.
- Gray TM and Matthews BW (1984) Intrahelical hydrogen bonding of serine, threonine and cysteine residues within alpha-helices and its relevance to membrane-bound proteins. *J Mol Biol* **175**:75–81.
- Guan X-M, Peroutka SJ, and Kobilka BK (1992) Identification of a single amino acid residue responsible for the binding of a class of β -adrenergic receptor antagonists to 5-HT_{1A} receptors. *Mol Pharmacol* **41**:695–698.
- Han M, Lou J, Nakanishi K, Sakmar TP, and Smith SO (1997) Partial agonist activity of 11-cis-retinal in rhodopsin mutants. *J Biol Chem* **272**:23081–23085.
- Ho BY, Karschin A, Branchek T, Davidson N, and Lester HA (1992) The role of conserved aspartate and serine residues in ligand binding and in function of the 5-HT_{1A} receptor: a site-directed mutation study. *FEBS Lett* **312**:259–262.
- Horn F, Weare J, Beukers MW, Hörsch S, Bairoch A, Chen W, Edvardsen Ø, Campagne F, and Vriend G (1998) GPCRDB: an information system for G protein coupled receptors. *Nucleic Acids Res* **26**:277–281.
- Hosmer DW and Lemeshow S (1989) *Applied Logistic Regression*. John Wiley & Sons, Inc., New York.
- Ji TH, Grossmann M, and Ji I (1998) G protein-coupled receptors. I. Diversity of receptor-ligand interactions. *J Biol Chem* **273**:17299–17302.
- Kelley LA, Gardner SP, and Sutcliffe MJ (1996) An automated approach for clustering an ensemble of NMR-derived protein structures into conformationally-related subfamilies. *Protein Eng* **9**:1063–1065.
- Kraulis J (1991) MOLSCRIPT: a program to produce both detailed and schematic plots of protein structure. *J Appl Cryst* **24**:946–950.
- Kumar S and Bansal M (1998) Geometrical and sequence characteristics of α -helices in globular proteins. *Biophys J* **75**:1935–1944.
- Liapakis G, Ballesteros JA, Papachristou S, Chan WC, Chen X, and Javitch JA (2000) The forgotten serine. A critical role for Ser-203^{5.42} in ligand binding to and activation of the β_2 -adrenergic receptor. *J Biol Chem* **275**:37779–37788.
- Lopez-Rodriguez ML, Morcillo MJ, Fernandez E, Porras E, Orensanz L, Beneytez ME, Manzanares J, and Fuentes JA (2001a) Synthesis and structure-activity relationships of a new model of arylpiperazines. 5. Study of the physicochemical influence of the pharmacophore on 5-HT_{1A}/ α_1 -adrenergic receptor affinity: synthesis of a new derivative with mixed 5-HT_{1A}/ D_2 antagonist properties. *J Med Chem* **44**:186–197.
- Lopez-Rodriguez ML, Morcillo MJ, Fernandez E, Rosado ML, Pardo L, and Schaper K-J (2001b) Synthesis and structure-activity relationships of a new model of arylpiperazines. 6. Study of the 5-HT_{1A}/ α_1 -adrenergic receptor affinity by classical Hansch analysis, artificial neural networks and computational simulation of ligand recognition. *J Med Chem* **44**:198–207.
- Lopez-Rodriguez ML, Rosado ML, Benhamú B, Morcillo MJ, Sanz AM, Orensanz L, Beneytez ME, Fuentes JA, and Manzanares J (1996) Synthesis and structure-activity relationships of a new model of arylpiperazines. 1. 2-[[4-(*o*-Methoxyphenyl)piperazin-1-yl]methyl]-1,3-dioxoperhydroimidazo[1,5-*a*]pyridine: a selective 5-HT_{1A} receptor agonist. *J Med Chem* **39**:4439–4450.
- Lowry OH, Rosebrough NJ, Farr AL, and Randall RJ (1951) Protein measurement with the folin phenol reagent. *J Biol Chem* **193**:265–275.
- Merritt EA and Bacon DJ (1997) Raster3D: photorealistic molecular graphics. *Methods Enzymol* **277**:505–524.
- O'Neil KT and DeGrado WF (1990) A thermodynamic scale for the helix-forming tendencies of the commonly occurring amino acids. *Science (Wash DC)* **250**:646–651.
- Oliveira L, Paiva ACM, Sander C, and Vriend G (1994) A common step for signal transduction in G-protein coupled receptors. *Trends Pharmacol Sci* **15**:170–172.
- Palczewski K, Kumasaka T, Hori T, Behnke CA, Motoshima H, Fox BA, LeTrong I, Teller DC, Okada T, Stenkamp RE, et al. (2000) Crystal structure of rhodopsin: a G protein-coupled receptor. *Science (Wash DC)* **289**:739–745.
- Pavia ML, Taylor CP, Hershenson FM, and Lobbsteal SJ (1987) 6-Alkoxy-N,N-disubstituted-2-pyridinamines as anticonvulsants. *J Med Chem* **30**:1210–1214.
- Scheer A, Fanelli F, Costa T, De Benedetti PG, and Cotecchia S (1996) Constitutively active mutants of the alpha 1B-adrenergic receptor: role of highly conserved polar amino acids in receptor activation. *EMBO (Eur Mol Biol Organ) J* **15**:3566–3578.
- Senes A, Gerstein M, and Engelman DM (2000) Statistical analysis of amino acid patterns in transmembrane helices: the GxxxG motif occurs frequently and in association with β -branched residues at neighboring positions. *J Mol Biol* **296**:921–936.
- Strader CD, Candelore MR, Hill WS, Dixon RA, and Sigal IS (1989) A single amino acid substitution in the beta-adrenergic receptor promotes partial agonist activity from antagonists. *J Biol Chem* **264**:16470–16477.
- Strader CD, Sigal IS, Candelore MR, Rands MR, Hill WS, and Dixon RAF (1988) Conserved aspartic acid residues 79 and 113 of the β -adrenergic receptor have different roles in receptor function. *J Biol Chem* **263**:10267–10271.
- Suryanarayana S, Daunt DA, Zastrow MV, and Kobilka BK (1991) A point mutation in the seventh hydrophobic domain of the α_2 -adrenergic receptor increases its affinity for a family of β receptor antagonists. *J Biol Chem* **266**:15488–15492.
- Suryanarayana S and Kobilka BK (1993) Amino acid substitutions at position 312 in the seventh hydrophobic segment of the β_2 -adrenergic receptor modify ligand-binding specificity. *Mol Pharmacol* **44**:111–114.
- Unger VM, Hargrave PA, Baldwin JM, and Schertler GF (1997) Arrangement of rhodopsin transmembrane alpha-helices. *Nature (Lond)* **389**:203–206.
- van Rhee AM and Jacobson KA (1996) Molecular architecture of G protein-coupled receptors. *Drug Devel Res* **37**:1–38.
- Yang K, Farrens DL, Attenbach C, Farahbakhsh ZT, Hubbell WL, and Khorana HG (1996) Structure and function in rhodopsin. Cysteines 65 and 316 are in proximity in a rhodopsin mutant as indicated by disulfide formation and interactions between attached spin labels. *Biochemistry* **35**:14040–14046.
- Yu H, Kono M, McKee TD, and Oprian DD (1995) A general method for mapping tertiary contacts between amino acid residues in membrane-embedded proteins. *Biochemistry* **34**:14963–14969.
- Zhou W, Flanagan C, Ballesteros JA, Konvicka K, Davidson JS, Weinstein H, Millar RP, and Sealfon SC (1994) A reciprocal mutation supports helix 2 and helix 7 proximity in the gonadotropin-releasing hormone receptor. *Mol Pharmacol* **45**:165–170.

Address correspondence to: Dr. Leonardo Pardo, Unitat de Bioestadística, Facultat de Medicina, Universitat Autònoma de Barcelona, 08193 Bellaterra (Barcelona), Spain. E-mail: leonardo.pardo@uab.es
